Wetting phenomena on external and internal interfaces in solids: common features and peculiarities

E.I. Rabkin, L.S. Shvindlerman, B.B. Straumal and O.I. Noskovich

Institute for Solid State Physics, Academy of Sciences of the USSR, Chernogolovka, Moscow district 142432, USSR

At the critical point of the β-γ' transition in a Sn-rich Sn–In alloy a discontinuity in the thermal dependence of the tin–indium interdiffusion coefficient has been observed. Similar, but shifted in temperature discontinuities have been observed during In diffusion along grain boundaries in tin and Sn–Ge interphase boundaries. The results obtained are explainable under the assumption that the prewetting phase transition occurs on the boundaries. Penetration of Zn along symmetrical [100] tilt grain boundaries in Fe–5at%Si and Fe–12at%Si alloys has been studied. Wetting of grain boundaries by the Zn-rich melt has been observed. The region behind the wetting film is observed to have an unusually high grain boundary diffusivity of Zn followed by the region of usual grain boundary diffusivity. Such a phenomenon may be explained in terms of the so-called premelting phase transition "GB-thin wetting film on the boundary". Grain boundary phase diagrams have been constructed.

1. Introduction

According to Cahn's consideration [1], in the vicinity of the miscibility critical point one can observe a wetting transition on the solid substrate. If the wetting transition is of the first order, the corresponding prewetting transition in a single-phase region may be observed. On the other hand, the thickness of the layer with distorted structure at the grain boundaries is approximately the same as at the external surface. So phase transitions on the surfaces and on the grain boundaries must have much in common. To investigate the wetting phenomena on the grain boundaries (GBs) and interphase boundaries we have taken Sn–In and Fe–Zn systems. In the former alloy at a temperature $T_c = 178°C$ the critical point of the β-γ' transition is observed [2], in the Fe–Zn alloy the line of the solubility limit in the solid solution based on bcc iron is placed very near to the metastable curve of solid solution decomposition, and the "virtual" critical point of this curve lies only a little above the peritectic temperature [3].

2. Experimental methods

To investigate the GBs and interphase boundaries properties in the Sn–In system we selected [001] twist boundaries. For investigation tin and tin–germanium bicrystals were grown by means of directed crystallization in a high-purity argon atmosphere. Tin bicrystals with misorientation angles of 27.6°, 28.1°, 29.0°, 30.2°, 31.1° and tin–germanium bicrystals with misorientation angles of 0°, 1°, 3°, 10° were grown. 99.999 at% pure tin and Sb–doped semiconducting germanium with a specific resistance of 5 Ω cm were used in the production of bicrystals (the growth technique has been described in ref. [4]).

The indium layer was electrolytically deposited on the surface of the bicrystals. The layer thickness was 100–200 μm. The samples were annealed in a high-purity argon atmosphere in a special furnace consisting of a thermostat and 12 small furnaces in which different temperatures were maintained [4]. The indium concentration distribution in the diffusion zones was determined by

means of electron microprobe analysis from the intensity of the In Lα line at an accelerating voltage of 15 kV.

The product of the grain boundary diffusion coefficient D' and the boundary width δ was determined by Fisher's method.

All experiments in the Fe–Zn system were carried out with GBs tilted 43° with respect to [100] of an Fe–5at%Si alloy and with Gbs tilted 38° with respect to [100] of an Fe–12at%Si alloy. Small additions of Si make it possible to grow Fe single crystals and bicrystals. The bicrystals were grown by the electron-beam zone melting technique in a vacuum of the order of 10^{-6} Torr with a growth rate of 1 mm/min. A layer of Zn was applied to the specimens by immersing them into the melt. Before immersion the specimens were mechanically ground followed by chemical polishing in a solution containing 80% H_2O_2 + 14% H_2O + 6% HF. The samples were annealed in the temperature range 652–975°C. The Zn concentration profiles were determined by means of electron probe microanalysis.

3. Results and discussion

3.1. Sn–In system

Fig. 1 presents the temperature dependence of the coefficient of the interdiffusion of indium in tin for indium concentrations in the range of 2 to 8at%In. At a temperature $T_c = 178.7 \pm 0.5°C$ this dependence exhibits a discontinuity. Above and below T_c the diffusion coefficient obeys the Arrhenius law. The temperature T_c coincides with the temperature of the critical point of the β–γ' transition in the Sn–In alloy [2].

Fig. 2 presents the temperature dependences of the product $D'\delta$ for five twist grain boundaries with different misorientation angles. Each of these dependences exhibits two regions: a high and a low-temperature one. At a certain temperature T_c^B the diffusion coefficient changes abruptly. These temperatures T_c^B are different for different boundaries and are by 17–25°C lower as compared to T_c for the bulk diffusion coefficient. At a temperature T_c of the bulk phase transition β–γ',
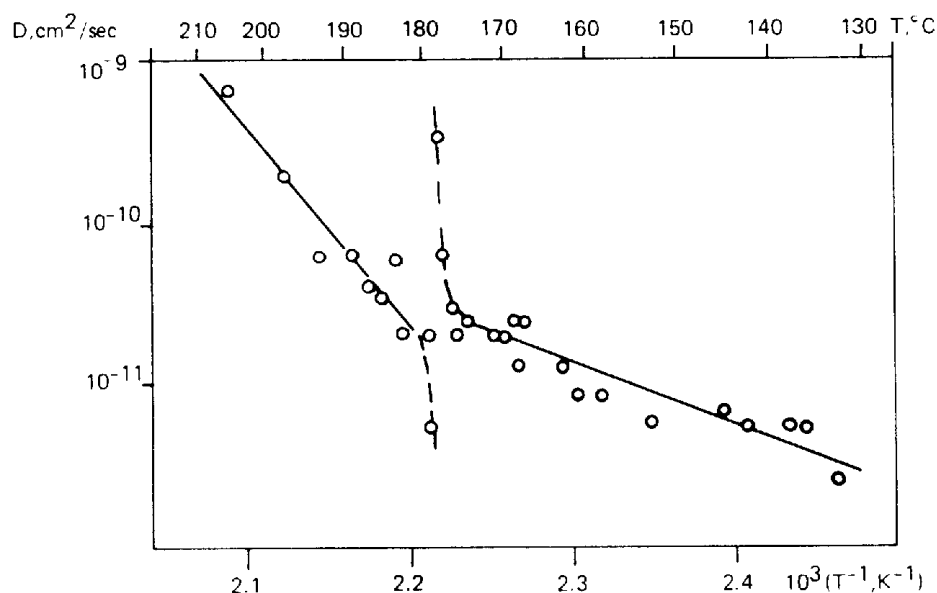

Fig. 1. Temperature dependence of the bulk diffusion coefficient of indium in the concentration range from 2 to 8at% In. The discontinuity in the temperature dependence at T_c corresponds to the β–γ' transition.

where an abrupt change of D is observed, the dependences $D'\delta(T)$ for grain boundaries exhibit no singularities.

The temperature dependences of the product $D'\delta$ are shown in fig. 3 for the four interphase twist boundaries studied. Each of these dependences exhibit a discontinuity at T_c^B. These temperatures differ for different boundaries. On approaching the T_c^B temperature from below, the values of $D'\delta$ are considerably higher than the Arrhenius plot values whereas on approaching T_c^B from high temperatures they are lower. The deviations are observed within the temperature range $T_c^B \pm 5\,°C$. This behaviour of the diffusion coefficient may be attributed to critical phenomena in the vicinity of the $\beta\gamma'$ phase transition in the bulk

Fig. 2. Temperature dependences of the product $D'\delta$ for boundaries with different misorientation angles ϕ: (1) 28.1°; (2) 29.0°; (3) 27.6°; (4) 30.2°; (5) 31.1°.

and in the boundaries. Note, that the T_c^B values for interphase boundaries are only 0–14°C lower as compared with the T_c temperature for the bulk diffusion coefficient.

We suppose that a prewetting phase transition occurs on the boundaries – on the grain boundary in the γ'-phase a thin equilibrium layer of the β-phase is formed at temperature for which the β-phase is unstable in the bulk. This hypothesis allows us to understand the basic features of the experimental results obtained.

(1) Due to distortion of the interatomic bounds at the GB the disordered β-phase is favored at the GB even below the temperature T_c of the $\gamma'-\beta$ transition in the bulk. So the temperature T_c^B is lower on the boundaries as compared with the bulk.

(2) At the temperature T_c there is a complete wetting of the boundary by the disordered β-phase, and $\gamma'-\beta$ transition in the bulk has no influence on the GB structure and the diffusional properties. So there are no singularities in the $D'\delta(T)$ dependences at the temperature T_c of the bulk $\beta-\gamma'$ transition.

In order to understand the nature of the difference in the diffusional behaviour of the grain boundaries and the interphase boundaries we will consider a lattice-gas model of the following kind (according to Pandit et al. [5]): the atoms occupy the sites of a semi-infinite homogeneous lattice placed on the substrate. We denote the potential of the nearest neighbour interaction by V, whereas the potential of the attraction of the atomic layer next to the substrate by the substrate is denoted by U. Under certain circumstances, this model undergoes a wetting transition. If the condition $0.7 \leqslant U/V \leqslant 0.9$ is satisfied, the wetting transition is of first order and a corresponding prewetting transition also exists. When the ratio U/V decreases (i.e. a lowering of the attractive potential of the substrate) then the temperature T_w of the wetting transition increases. If $U/V \leqslant 0.7$, a second-order wetting transition occurs, with a strongly developed fluctuation phenomenon.

The tin bicrystal may be considered as a semi-infinite single crystal placed on a substrate formed by another single crystal misoriented with respect to the first one. In such a presentation, the poten-
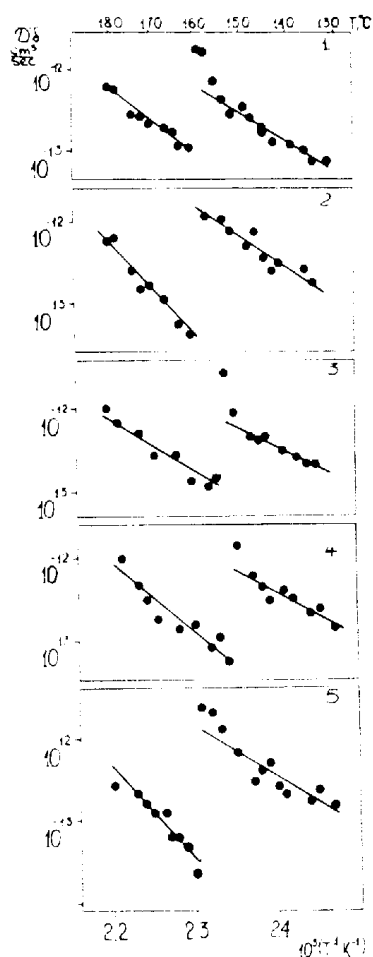
tial U is strong enough to be comparable with the energy of the interatomic interaction in the lattice. Indeed, the temperatures of the grain boundary phase transition were found to be considerably lower than that for the bulk: the temperature dependences of the grain boundary diffusion coefficient exhibited large gaps. The latter finding indicated quite definitely that we are dealing with a first-order transition.

In the case of the Sn–Ge interface the absence of any solubility in the Sn–Ge system means that the potential of the Sn–Ge interaction is considerably lower than that of the Sn–Sn or Ge–Ge interactions; i.e. the ratio U/V is low. According to Pandit's scheme this means that the temperature T_c^B of the boundary transition on the interphase boundaries must be higher than on the GBs, and the transition itself must be close to the second-order phase transition with strongly developed fluctuations. All this can be clearly seen from figs. 2 and 3.

3.2. Fe–Si–Zn system

To estimate $D'\delta$ a sequence of concentration profiles perpendicular to the GB and parallel to the sample surface has been measured, and the c_b values have been calculated from the maxima of these profiles corresponding to the GB position. The $D'\delta$ values can be determined from the slope of the variation of log c_b against the depth y. These log $c_b - y$ plots for different temperatures in the case of the Fe–5at%Si alloy are displayed in fig. 4. These plots consist of an initial part having a low gradient followed by a steep slope. The concentration c_{Bt} (the concentration at which $D'\delta$ changes) has been obtained from the point of intersection of these two parts having different slope. From the experimental evidence in fig. 4 it may be suggested that a phase transition accompanies the formation of the thin wetting layer at c_{Bt} near the GBs. At the intersection points in fig. 4, the GB thickness may increase abruptly. As-
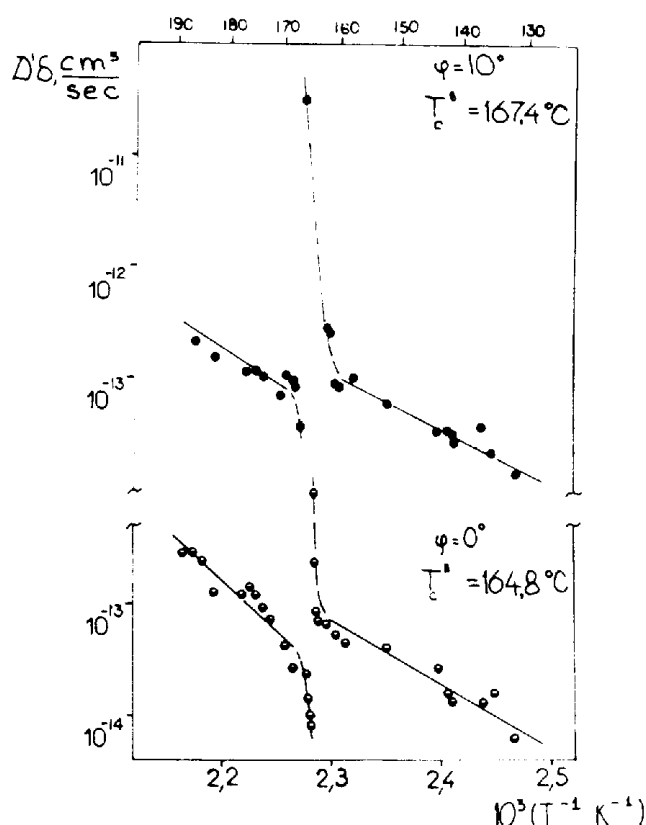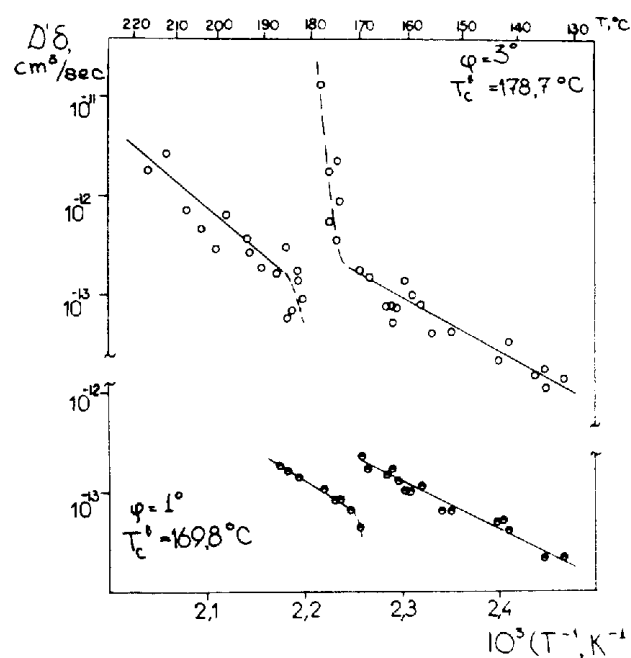

Fig. 3. Temperature dependences of the product $D'\delta$ for four twisted [001] Sn–Ge interphase boundaries. The misorientation angles and temperatures of the β–γ' phase transitions on the boundaries are shown.
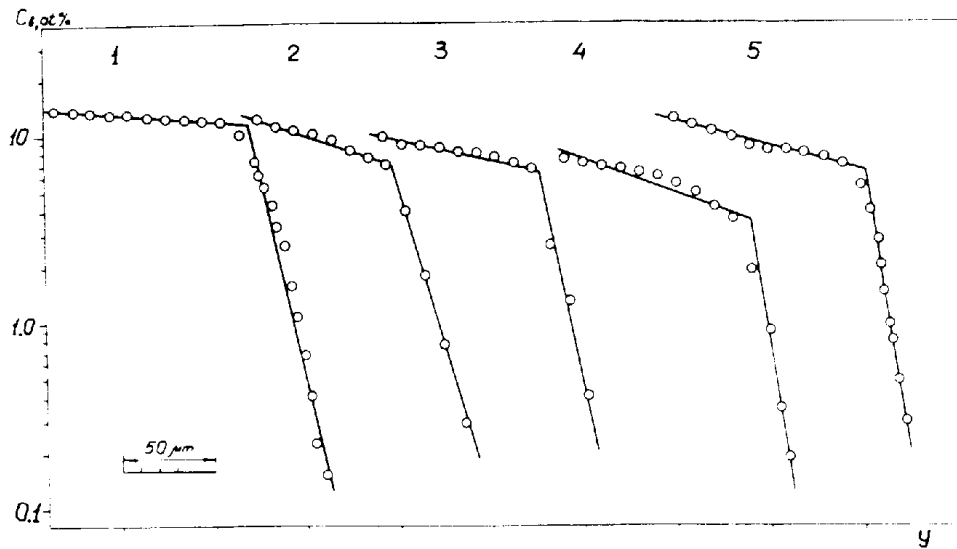
Fig. 4. Dependences of the zinc concentration of the boundaries c_B on the depth y for different temperatures in the Fe-5at%Si alloy. At the concentration c_{Bt}, the value of the product of the diffusion coefficient and the boundary width $D'\delta$ is changed abruptly. The product is measured by the slope of the $c_b(y)$ dependence. The c_{Bt} concentration is changed with temperature. (1) 975°C, 1.75 h; (2) 857°C, 7.5 h; (3) 809°C, 21 h; (4) 790°C, 63 h; (5) 745°C, 102 h.

suming D' constant above an below c_{Bt}, the wetted GB thickness δ can be estimated from $D'\delta$ above and below c_{Bt}. The value of δ so obtained is approximately 10^2. It is important to mention that

the GB wetting by the Zn-rich melt (a thin, $\cong 1$ μm layer enriched in Zn along the GB) is observed at all temperatures studied.

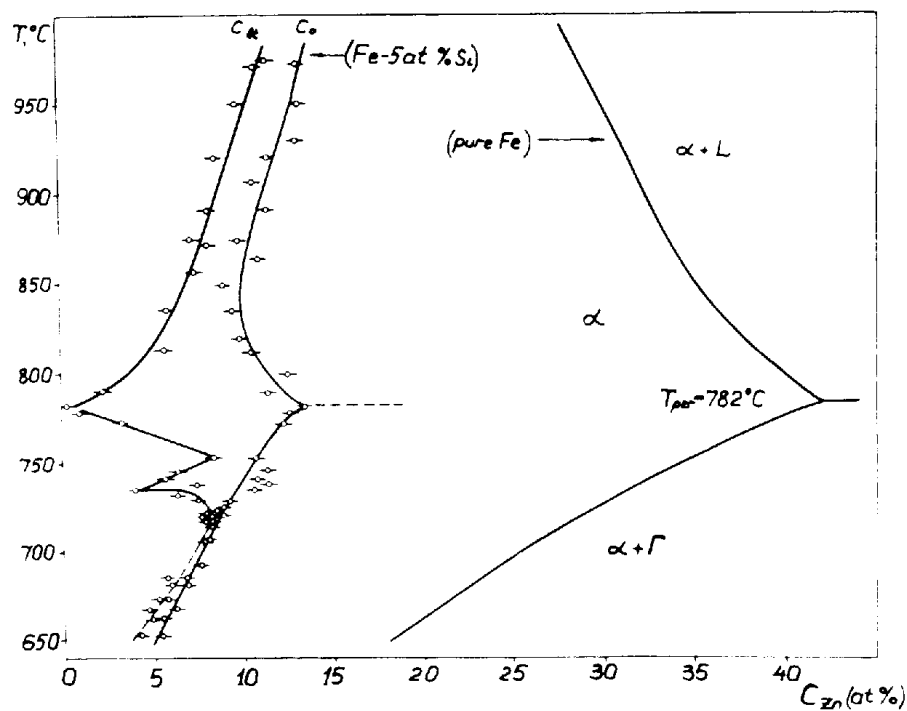The temperature dependence of c_{Bt} for the

Fig. 5. Thermal dependences of c_{Bt} and c_0 in the Fe-5at%Si alloy. The zinc concentration is plotted on the x-axis. The line of the solubility limit of zinc in pure iron is also displayed (solidus and solvent line).
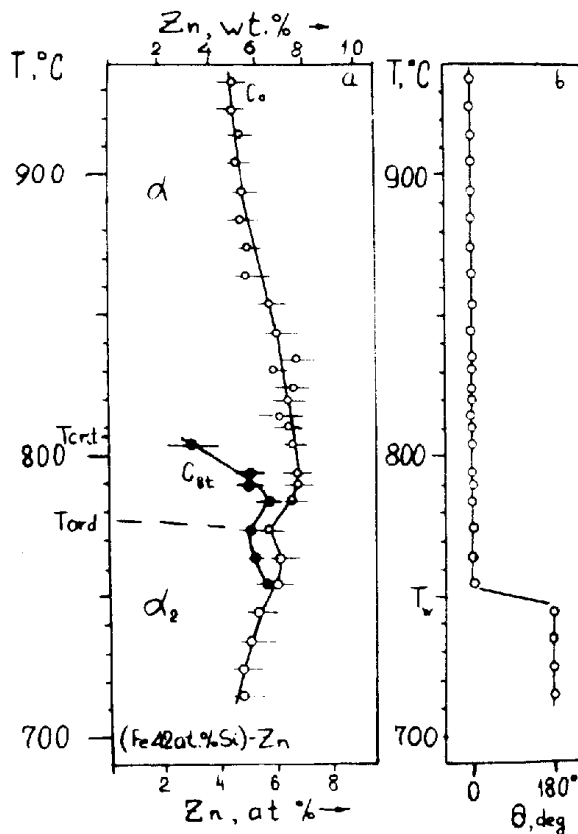
Fig. 6. (a) Phase diagram of the system Fe–12at%Si–Zn. T_{ord} is the temperature of bulk ordering A_2–B_2; T_{crit} is the critical point on the line $c_{Bt}(T)$ of grain boundary premelting transition. (b) Temperature dependence of the angle θ in the site of the grain boundary intersection with the surface. T_w is the temperature of the grain boundary wetting transition.

Fe–5at%Si–Zn alloy is displayed in fig. 5. In this figure, the line of the solubility limit of zinc in the Fe–5at%Si alloy according to our data and that of zinc in pure iron from the literature are displayed. The maximum of solubility is observed at the peritectic temperature. The $c_{Bt}(T)$ line has a rather complicated form. Above the Curie point the c_{Bt} value is the lower, the greater is the bulk solubility limit c_0. In the vicinity of the Curie point this correlation is distorted: the line has a protuberance faced to the lower zinc concentrations.

In fig. 6a, the phase diagram for the Fe–12at%Si–Zn alloy is presented. White points indicate the values of the bulk solubility limit of zink in the Fe–12at%Si alloy (solvent line). Black points

correspond to the values of concentration c_{Bt}, at which the knees on the curves $c_b(y)$ are observed, and the diffusion permeability of the grain boundaries undergoes an abrupt change. At the temperature T_w the wetting transition occurs. This can be clearly seen from fig. 6b, where the thermal dependence of the angle θ in site of the GB intersection with the solid–melt interface is displayed. It can be clearly seen from fig. 6a, that the $c_{Bt}(T)$ line unites with the solvent line $c_0(T)$ at the temperature T_w. In fact, at this temperature the wetting of the grain boundaries and the gentle region on the zinc grain boundary diffusion curves $c_b(y)$ disappear simultaneously. Above T_w, the $c_{Bt}(T)$ line gradually goes away from the solvent line $c_0(T)$ and finishes at a temperature $804°C < T < 810°C$. At $804°C$, the penetration curve $c_b(y)$ still contains a knee, while at $T = 810°C$ this knee is absent, although the penetration curve has some traces of steep and smooth regions. In the vicinity of the bulk ordering temperature, protrusions directed towards the region of low concentrations can be seen on the line $c_{Bt}(T)$ and the solvent line $c_0(T)$.

All the features of the grain boundary phase diagrams observed may be understood in terms of the so-called premelting phase transition "GB → thin wetting film on the boundary". Details of this calculation will be presented in ref. [6].

References

[1] J.W. Cahn, J. Chem. Phys. 66 (1977) 3667.
[2] E.I. Rabkin, L.S. Shvindlerman and B.B. Straumal, J. Less-Common Metal. 158 (1990) 23.
[3] O. Kubaschewski, Iron-Binary Phase Diagrams (Springer, Berlin);
    Verlag Stahleisen mbH. Düsseldorf, 1982.
[4] E.L. Maksimova, B.B. Straumal, V.E. Fradkov and L.S. Shvindlerman, Fiz. Met. Metalloved. 56 (1983) 979.
[5] R. Pandit, M. Schich and M. Wortis, Phys. Rev. B 26 (1982) 5112.
[6] O.I. Noskovich, E.I. Rabkin, V.N. Semenov, L.S. Shvindlerman and B.B. Straumal, Acta Metal., submitted.